Mean-field simulation of metal oxide antiferromagnetic films and multilayers

M. Charilaou* and F. Hellman

Department of Physics, University of California, Berkeley, California 94720-7300, USA

(Received 9 February 2013; revised manuscript received 10 May 2013; published 31 May 2013)

In this work the magnetization in antiferromagnetic thin films and multilayers with interlayer exchange coupling is simulated using mean-field approximation. Transition-metal oxide antiferromagnets are modeled as multiplane magnetic systems with 1 to 11 planes and the magnetization M is calculated as a function of temperature T. The antiferromagnetic films exhibit ferromagnetism when the number of monolayers is odd, i.e., when there is an uncompensated plane, but the net magnetization is lower than that of any single uncompensated plane due to cancellations and finite-size effects. With increasing film thickness the Néel temperature increases monotonically and the magnetic moment near the surface is reduced compared to that of the core, changing the form of the $M(T)$ curve. When antiferromagnetic films are exchange coupled to each other, as in a multilayer with a nonmagnetic intervening layer, the surface magnetization of each film increases and the ferromagnetism of odd-numbered systems is enhanced. These results are shown to be experimentally testable by comparing magnetometry and neutron diffraction.

DOI: 10.1103/PhysRevB.87.184433 PACS number(s): 75.10.Hk, 75.40.Mg, 75.47.Lx, 75.50.Ee

I. INTRODUCTION

The magnetization and ordering temperature of thin magnetic films have been studied extensively because of their technological importance and due to fundamental interest in new phenomena which emerge at the nanoscale. While finite-size effects most often reduce the magnetic properties of thin films, in metallic ferromagnetic (FM) films, with the exception of Ni on Cu, the magnetic moments at the surface or interface are larger than in the bulk[1–5] due to band narrowing at the surface and a large density of states (DOS) at the Fermi level.[3] In contrast, antiferromagnetic (AFM) metal oxide films (MO) have localized magnetic moments and their DOS at the Fermi level is zero; therefore, the formation of surface states, and thus the enhancement of surface magnetism, is not expected.[6] This was shown for Heisenberg antiferromagnets, where the ordering temperature increases monotonically with increasing film thickness,[7] and the surface magnetization is reduced compared to the film core in the absence of quantum fluctuations.[8]

The magnetic properties of oxide antiferromagnetic films have been increasingly investigated,[9–12] especially after the discovery of exchange bias[13] and giant magnetoresistance.[14] Oxides of the transition metals Mn, Fe, Co, and Ni are antiferromagnetic with Néel temperatures of[15–18] $T_N \approx 120$ K for MnO, 200 K for FeO, 300 K for CoO, and 520 K for NiO. Below T_N, spins are ferromagnetically coupled within (111) planes of the NaCl structure and antiferromagnetically coupled to neighboring planes[17] and, with the exception of FeO, the magnetization lies predominantly inside the (111) plane.[17] This magnetic configuration in MO AFM thin films, in which alternating planes cancel each other out, leads to a dominance of uncompensated spins, which may be coupled to the Néel vector or not, in the measured magnetization of such systems. Recently, this aspect was exploited and it was experimentally shown that AFM multilayers can be used as a source of ferromagnetism, arising from uncompensated magnetization coupled via a lightly doped semiconductor, in a new type of magnetic semiconductor.[19] The findings of that work motivated this theoretical investigation. Identifying the mechanisms which govern the magnetization in such systems is crucial to fully understand and predict the behavior of exchange biased films and exchange-coupled multilayers of magnetic semiconductors with uncompensated AFM films. The magnetization properties in such systems are dominated by finite-size effects which reduce the magnetic moment near the surface, thus generating a magnetization profile as a function of film thickness. While the magnetization profiles in thin ferromagnetic films have been studied extensively,[20–23] the effect of finite size on the magnetization of AFM films is not known.

In this work we therefore present a theoretical study of AFM films and multilayers using a simple mean-field model for a metal oxide in the NaCl structure, where the system consists of ferromagnetically ordered (111) planes which are antiferromagnetically coupled to each other. We chose to use the mean-field method because it is the most suitable approach for the description phase transitions in systems with many sublattices, as in the case of the AFM films, where each atomic plane is treated as a sublattice to obtain the magnetization profile. Our focus lies on the magnetization profile as a function of thickness and its impact on the net magnetization in thin AFM films. While it is intuitive that uncompensated AFM films, i.e., with odd number of atomic planes, exhibit nonzero magnetization, in Sec. III it will be seen that the net magnetization of an uncompensated AFM film is, surprisingly, not equal to the magnetization of any single uncompensated plane.

II. THEORETICAL MODEL

Let us consider the Hamiltonian of the system, in which spins interact with their nearest neighbors, and with an external field:

$$\mathcal{H} = -\frac{1}{2}\sum_{i}^{N}\sum_{j}^{z} J_{ij} S_i S_j - h\sum_{i}^{N} S_i. \qquad (1)$$

The spin S represents the localized total angular momentum, J_{ij} is the exchange coupling constant between S_i and S_j, and

h is the external field. The sum over i runs to the total number of spins N and the sum over j runs to the number of nearest neighbors z of each spin S_i.

Considering the sheetwise ordering of MO inside the (111) planes, we divide the system into alternating planes. In a system with D planes, each containing N_d ions, the first term of the Hamiltonian can be broken down to account for interactions within the same plane d with coordination number z via exchange constant J and interactions with the spins in the neighboring planes with coordination number z^* via an interplane exchange constant J^*, which we scale with J, i.e., $J^* = \alpha J$. The Hamiltonian for each plane d then reads

$$\mathcal{H}_d = -\frac{1}{2}\sum_{i}^{N_d}\left[\sum_{j}^{z} J S_{d,i} S_{d,j} + \sum_{j}^{z^*} J^* S_{d,i}(S_{d+1,j}+S_{d-1,j})\right] - h\sum_{i}^{N_d} S_{d,i}. \quad (2)$$

The Hamiltonian of the entire system is then the sum of all planes: $\mathcal{H} = \mathcal{H}_1 + \cdots + \mathcal{H}_d + \cdots + \mathcal{H}_D$. We simplify the Hamiltonian in Eq. (2) using the Weiss mean-field approximation (MFA), i.e., by introducing the magnetization $m_d = \langle S_d \rangle$ which corresponds to the mean field in the dth plane. The strength of the mean field depends on the number of neighbors, i.e., z and z^*, which in the ABC stacking of (111) planes in the NaCl structure is 6 and 3, respectively. The MFA treatment decouples all the spins and reduces the Hamiltonian to that of a single spin for each plane:

$$\mathcal{H}_d^{\mathrm{MFA}} = \underbrace{\frac{N_d}{2}\left[z J m_d^2 + z^* J^* m_d (m_{d+1}+m_{d-1})\right]}_{X_d} - \underbrace{\left[z J m_d + h + z^* J^* (m_{d+1}+m_{d-1})\right]}_{Y_d}\sum_{i}^{N_d} S_{d,i}. \quad (3)$$

The partition function $Z(T)$ and the equation of state for the above Hamiltonian can be obtained after choosing the type of spins. Heisenberg-type spins have $S(S+1)$ possible values and the equation of state for the z projection is the Brillouin function,[5] but low-dimensional systems with isotropic exchange exhibit no long-range order.[24,25] In contrast, Ising systems have infinite anisotropy, where Ising-type spins can only take $\pm S$ values and the equation of state is of the form[26,27]

$$m_d = |S| \tanh(|S|\beta Y_d) = f(m_{d-1}, m_d, m_{d+1}), \quad (4)$$

with β the inverse temperature $1/T$ and $|S|$ the absolute spin value which is set to 2, i.e., the value for Co^{+2} spins ($\mu_{Co^{+2}} \approx 3.8\mu_B$).[17] We choose to use Ising spins in our calculations because CoO behaves more like an Ising system due to its high anisotropy.[11,28,29] Moreover, we scale all the energy contributions, i.e., the temperature T and the external field h with the intraplane exchange constant J. For the interplane exchange we use values of $\alpha = -0.5$, -1.0, and -1.5. While the most common choice for α for CoO would be[30] -2 or -3, our choice of parameters is directed towards a general description and understanding of this type of AFM system, where the ratio α is the dominant mechanism for finite-size effects, as will be seen below.

For the order parameters we define the net magnetization $M(T)$ of the system and the average absolute value of plane magnetization $|m(T)|$:

$$M(T) = \sum_{d=1}^{D} m_d(T), \quad (5a)$$

$$|m(T)| = \frac{1}{D}\sum_{d=1}^{D} |m_d(T)|. \quad (5b)$$

In the discussion each plane magnetization is normalized to 1 at $T = 0$, i.e., divided by $|S| = 2$ which is the magnetic moment per atom in the plane.

Finally, we derive the ordering temperature of a system with $D = 1$ (2 dimensions) and $D = \infty$ (3 dimensions) by expanding Eq. (4) for $h = 0$ and small plane magnetization ($|m| \to 0$). The two-dimensional system orders at $T_N = zJS^2$, and the three-dimensional system at $T_N = S^2 J(z + 2\alpha z^*)$. The thickness dependence of the ordering temperature within MFA is[31]

$$T_N(D) = \frac{S^2 J(z+2\alpha z^*)}{2}\left(1 + \cos\frac{\pi}{D+1}\right). \quad (6)$$

Considering the ordering temperature of bulk CoO ($T_N \approx 300$ K), and the coordination numbers $z = 6$ and $z^* = 3$, the exchange constant amounts to $J = 12.5/(1+\alpha)$ K. This value corresponds to $J = 0.55$ meV (for $\alpha = 1$), which is very close to results from quantum chemical *ab initio* calculations for CoO[30] (normalizing their value of 6.5 meV by a factor of 16 due to the use of $|S| = 1/2$ against our $|S| = 2$).

We next expand our model to simulate multilayers of MO films each with D planes, separated by a spacer layer (S) which allows interlayer exchange interactions. In this context, the interlayer coupling could be of any nature, including Ruderman-Kittel-Kasuya-Yosida (RKKY), dipolar, etc.; for an RKKY-type interaction, as suggested in Ref. 19, the spacer needs to have sufficient charge carrier density to facilitate such an interaction, as shown experimentally for CoO/Al-ZnO multilayers, where the RKKY-type IEC is mediated by the electrons of the Al dopants.[19] In that case, the interlayer coupling J_{IEC} between two surfaces, or sheets of spins, oscillates with the spacer layer thickness, and decays with[32] $J_{IEC} \propto e^{-L_S/\lambda}/L_S^2$, with L_S the thickness of the spacer layer, and λ the material-specific exchange decay length. We incorporate J_{IEC} in our model by coupling the top and bottom plane of the film with J_{IEC}, as shown in Fig. 1, effectively a type of periodic boundary condition. This corresponds to a stacking of multiple MO films, where the top plane of a film interacts with the bottom plane of the next one and so on. In this context of IEC-induced boundary conditions, when the energy contribution of IEC conflicts with that of J^*, the unit cell of the model needs to be doubled, i.e., to account for the modulation of the exchange constants (see discussion).

In the equation of state this energy contribution has the same form as that of the interplane exchange J^*, where the coordination number is set to 1, which means that Y_d [see Eq. (3)] in the equation of state for the bottom and the top

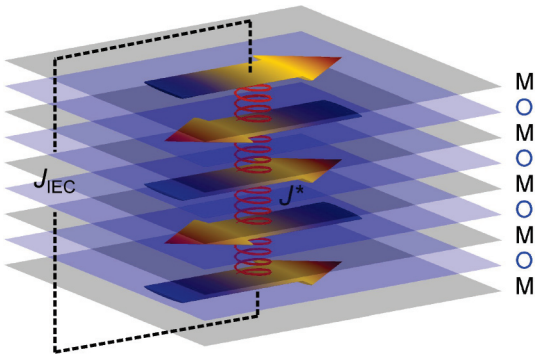

FIG. 1. (Color online) Illustration of the layered structure of an antiferromagnetic film with five planes. Alternating (111) planes of the NaCl structure are completely filled with metal ions (M) and oxygen (O) consecutively. The arrows inside the M planes indicate the alternating direction of the plane magnetization and the red springs correspond to the interplane exchange coupling J^*. The simulation of multilayers is performed by coupling the top and the bottom planes as indicated by the J_{IEC} bond.

planes in a film will have the form

$$Y_1 = zJm_1 + h + z^*J^*m_2 + J_{IEC}m_D, \tag{7a}$$

$$Y_D = zJm_D + h + z^*J^*m_{D-1} + J_{IEC}m_1. \tag{7b}$$

As with the other energy terms, we scale J_{IEC} with J and try different values which would correspond to a spacer with a few monolayers thickness, assuming a constant decay length λ of 10 monolayers ($J_{IEC} = 0.2J$ and $0.4J$).

The equations of state for all planes [Eq. (4)] must be solved simultaneously in order to find the magnetization of each plane at a temperature T and field h, from which we will obtain the magnetization of the entire film or multilayer. We therefore need to minimize

$$E = \sum_{d=1}^{D}[m_d - f(m_{d-1},m_d,m_{d+1})]^2 = 0. \tag{8}$$

This is done numerically by iterating all plane magnetizations by one of three possible changes, $+\delta$, 0, or $-\delta$, at the same time and checking which set of changes leads to the minimum of Eq. (8). This means that for D planes, D equations of state need to be solved at the same time, and each step towards the solution contains 3^D possibilities, which are all considered at each temperature step.

The accuracy of the solution of Eq. (4) depends on the step size δ and the value of E. In our simulations we vary the magnetization of each plane by $\delta = 10^{-5}|S|$ and require that $E \leqslant 10^{-6}$ is satisfied. This provides a very high resolution for the magnetization values and a high accuracy for the solution of the equations of state.

Using this procedure we simulate $M(T)$ curves for films with various thicknesses (D), interplane (J^*), and interlayer (J_{IEC}) exchange constants.

III. RESULTS AND DISCUSSION

We calculated the plane magnetization of systems with $D =$ 1 to 11, considering free films, i.e., with $J_{IEC} = 0$. For systems with even number of planes, all magnetization contributions are canceled out because the system is fully symmetric. For odd number of planes, however, there is one uncompensated plane, which results in a nonzero magnetization of the system, as expected according to Néel.[33] As will be seen later, however, the net magnetization is not equal to the magnetization of any single uncompensated plane.

Figure 2(a) shows the net film magnetization $M(T)$ (solid lines) and the average absolute value of plane magnetization $|m(T)|$ (dashed lines) of systems with odd number of planes as a function of temperature. For the simplest system with one plane ($D = 1$), there is no interplane exchange and the system represents a typical MFA Ising ferromagnet with ordering temperature $T_N = 150$ K. With increasing D, the ordering temperature increases monotonically and approaches saturation after a few planes [see Fig. 2(b)], following Eq. (6). For the system with $D = 11$ the ordering occurs at $T_N(11) = 0.983T_N(\infty)$.

This behavior of the ordering temperature is very similar to that of Heisenberg-type ferromagnetic EuO films,[5,22] and comparable to experimental observations in CoO/SiO_2 multilayers[11,12] and CoO/MgO and NiO/MgO superlattices.[10] The experimental values for the ordering temperature of CoO with a thickness of 6 and 10 atomic planes in Ref. 10 were 255(5) K and 275(5) K, respectively, which is in very good agreement with the MFA predicted values of $0.95T_N(\infty) \approx$ 270 K and $0.98T_N(\infty) \approx 280$ K, for the corresponding thicknesses (considering that the bulk value of that sample was 285 K). The monotonic increase of T_N differs, however, from that of metallic FM films, where the Curie temperature sometimes exceeds the bulk value due to the effect of surface electronic states,[34–37] which marks a clear distinction between metallic and oxide magnets.

Figure 2 further shows that with increasing thickness the shape of the $M(T)$ curve departs strongly from the Brillouin-like shape of $D = 1$ and the difference between net film magnetization $M(T)$ and average absolute plane magnetization grows surprisingly large (up to 40% for $D = 11$ at $T = 3T_N/4$), due to the different magnetization of different planes. As an example, for $D = 11$ the magnetization starts at a plateau for low temperature and then decreases in a nearly linear fashion with increasing temperature, until it reaches T_N.

The changes in $M(T)$ become increasingly smaller with increasing D and show no significant changes for $D \geqslant 7$. This becomes clear if we compare the normalized $M(T)$ curves of $D = 7$, 9, and 11, which have the same shape [see Fig. 2(c)]. The evolution of $M(T)$ with D is comparable to the evolution of the ordering temperature, which approaches saturation for $D \geqslant 7$. This means that if we keep increasing D the $M(T)$ curve will not change further, and the ordering temperature will eventually reach the bulk value.

While it may seem counterintuitive that the thinnest film behaves most like a mean-field magnet [with a Brillouin-function-like $M(T)$], this is due to a combination of finite-size effects plus the fact that this is an AFM where the magnetization of almost all planes is compensated. The effect of finite size is further investigated by observing the individual plane magnetizations. Figure 3 shows the plane magnetization for systems with $D = 4$, 5, 10, and 11 as a function of temperature. As seen in the figure, the plane magnetization at low temperature ($T \leqslant 0.4T_N$) is saturated for all planes,

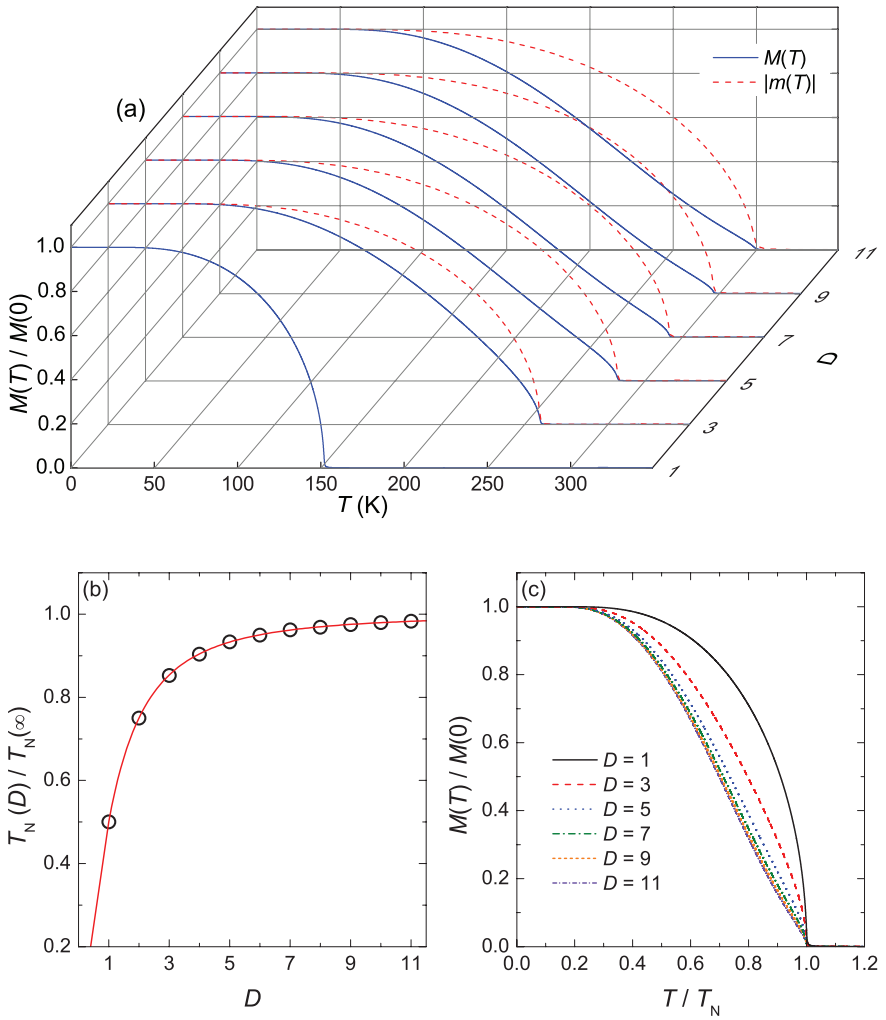

FIG. 2. (Color online) (a) Magnetization of systems with odd number of monolayers as a function of temperature. Solid lines correspond to the net film magnetization $M(T)$ and dashed lines correspond to the average absolute plane magnetization $|m(T)|$. (b) Evolution of the ordering temperature T_N as a function of D; the solid line corresponds to Eq. (6). (c) Normalized $M(T)$ curves as a function of T/T_N. With increasing D the $M(T)$ curve departs from the Brillouin-like shape and becomes nearly linear in the range $0.5 \leqslant T/T_N \leqslant 1.0$.

but for intermediate temperatures ($0.4T_N \leqslant T \leqslant 1.0T_N$) it differs strongly between surface and core planes. The surface planes have the weakest magnetization because they have a smaller number of interactions compared to the core of the film. The planes directly below the surface also have reduced magnetization because they are affected by the weaker magnetization of the outer planes. Planes which are two or more monolayers below the surface also exhibit some differences, which are however increasingly small. Similar magnetization profiles have been seen for antiferromagnetic Heisenberg EuTe(111) films, which exhibit strong finite-size effects, notably near $T \approx 0.5T_N$.[38]

For even-numbered systems [see Figs. 3(a) and 3(c)] all the plane magnetizations are canceled out because the system is fully symmetric: equal number and equal absolute value of magnetization points in positive and negative direction, respectively. For odd-numbered systems, however [see Figs. 3(b) and 3(d)], the surface planes add to each other, the next two add to each other and subtract from the top two, etc., generating the net film magnetization seen in Fig. 2. The net magnetization, notably, is not equal to the magnetization of any single uncompensated plane, but is lower at all intermediate T. This is because the magnetization in the positive direction, i.e., in the outer planes, changes differently with temperature compared to the magnetization in the negative direction, i.e., in the core planes, thus resulting in a strongly reduced and modified $M(T)$ curve.

We now test the effects of the interplane exchange coupling J^* by simulating the system with $D = 11$ for weaker ($\alpha = -0.5$) and stronger ($\alpha = -1.5$) coupling, and also consider ferromagnetic cases with $\alpha = +0.5$, $+1.0$, and $+1.5$.

Figure 4 shows the comparison of $M(T)$ curves for the six different J^* values, (a) showing the AFM and (b) the FM case. Considering first the AFM ($J^* < 0$) results, with decreasing α ratio the shape of the $M(T)$ curve changes and the curve becomes closer to the Brillouin-like shape of the MFA ferromagnet seen in the $D = 1$ film. The reason for this behavior is that, with decreasing strength of J^*, the difference in energy between near-surface and core planes is reduced. In the limit of $J^* \to 0$, the system with $D = 11$ will behave as 11 decoupled ferromagnets with an ordering temperature of the two-dimensional (2D) system and a Brillouin-like $M(T)$ curve. In contrast, if we increase J^* the energy difference becomes larger: near surface planes are increasingly weaker compared to the core planes and the $M(T)$ curve is modified further.

These observations are also valid in the ferromagnetic case [Fig. 4(b)]. The individual plane magnetizations $m(T)$ [see inset to Fig. 4(b)] of a ferromagnetic film with $D = 11$

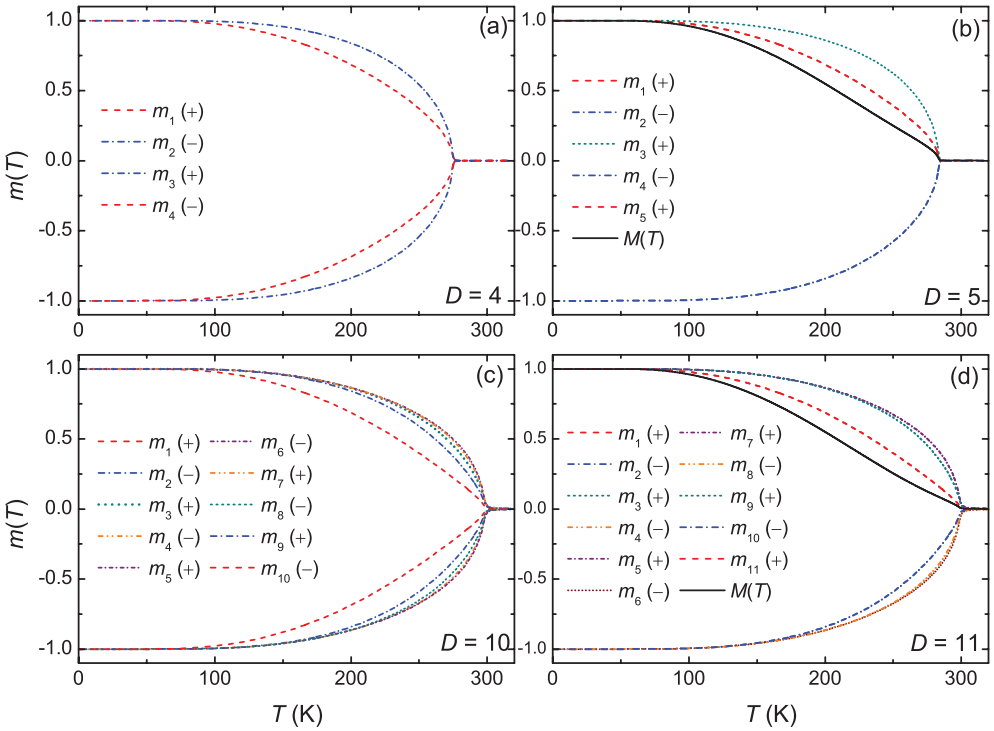

FIG. 3. (Color online) Plane magnetization of the systems with (a) $D = 4$, (b) 5, (c) 10, and (d) 11 as a function of temperature. The surface planes [e.g., 1 and 4 or 5 in (a) and (c), and 1 and 10 or 11 in (b) and (d)] have weaker magnetization compared to the core planes. For even number of monolayers the magnetization is fully symmetric ($m_{\text{odd}} = -m_{\text{even}}$) and the net sum $M(T)$ is zero (not shown), whereas for odd-numbered systems the surface magnetization is uncompensated and results in a net nonzero magnetization ($m_{\text{odd}} \neq -m_{\text{even}}$), shown as a solid line marked $M(T)$ in the right panels. Note that $M(T)$ is lower than the magnetization of any single uncompensated plane at intermediate temperatures.

(with $\alpha = 1$) are exactly the same as the individual plane magnetizations $|m(T)|$ of the AFM system shown in Fig. 3(d). The ordering temperature of the FM is also the same as in the AFM case, but since all plane magnetizations are positive, the shape of the net magnetization $M(T)$ for $D = 11$ is only very slightly modified from the Brillouin form of the $D = 1$ limit, in contrast to the case of AFM systems, and it is not strongly affected by the α ratio.

In the next step, we simulate multilayers of antiferromagnetic films each with $D = 11$ separated by nonmagnetic layers by using a single $D = 11$ film and turning on an interlayer exchange coupling J_{IEC}, as shown in Fig. 1, and investigate its effect on the behavior of the system. We assume that the IEC only acts on the surface planes, consistent with the assumption throughout this paper of nearest neighbor exchange only, and with the nature of the superexchange coupling of MO AFM's given the insulating nature of the MO layers. We test its effects for $J_{\text{IEC}} = 0.2J$ and $0.4J$, keeping $\alpha = -1$ for this set of simulations.

Figure 5 shows the net magnetization $M(T)$ as a function of the reduced temperature. The black solid line shows $M(T)$ of the uncoupled film ($J_{\text{IEC}} = 0$). The ordering temperature does not change with increasing interaction energy, but the shape of the $M(T)$ curve changes markedly. Positive coupling between films increases the magnetization of the surface planes and reverses the effects of finite size discussed above. In fact, if we consider the, unrealistic, limit of $J_{\text{IEC}} = |z^* J^*|$, the periodic boundary condition is complete and finite-size effects disappear: all planes have exactly the same magnetization and there is no distinction between surface and film core because all planes have the same number of bonds with the same bond strength, which corresponds to the case of $D \to \infty$.

For negative J_{IEC} the exact same effect occurs; the near-surface magnetic moments are enhanced. For this calculation we used two films instead of one, and coupled the bottom plane of the first to the top plane of the second, because the negative IEC doubles the unit cell of the system. In this case the net magnetization of each film is antiparallel to that of its two neighboring films in the multilayer (data not shown), resulting in a zero magnetization of the multilayer, as seen experimentally for CoO/Al-ZnO multilayers.[19]

For systems with an even number of atomic planes, the effect of IEC (whether positive or negative) is the same, i.e., the magnetic moment near the surface at intermediate temperatures is enhanced. In this case, positive or negative IEC affects the direction of individual planes at the top and bottom of each layer, but the net magnetization of each film and in turn of the multilayer, however, is always zero because all individual plane magnetizations cancel each other out.

In addition to IEC, an external field can influence the ordering of an AFM film or multilayer. When we apply an external field h on the AFM films, the shape of the $M(T)$ curve is drastically changed and the ordering is strongly affected: the onset of magnetization at T_{N}, which remains unchanged, becomes increasingly smeared with stronger h (see inset to Fig. 5) due to paramagnetic effects above T_{N}. The presence

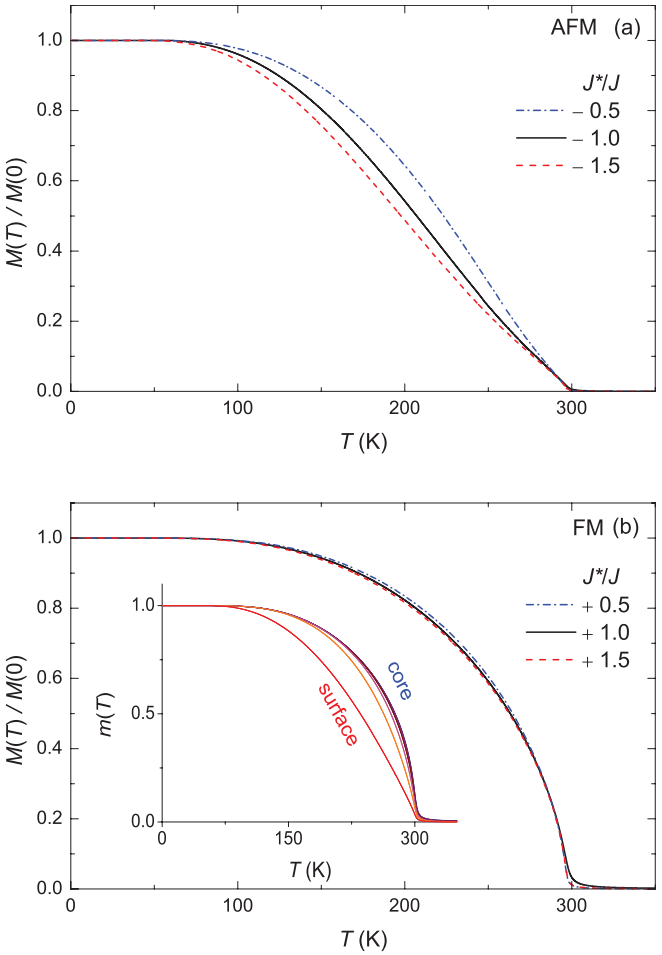

FIG. 4. (Color online) Net magnetization of the system with $D = 11$ as a function of temperature. The three different calculations correspond to cases where $\alpha = J^*/J = -0.5$ (dash-dotted blue line), -1.0 (solid black line), and -1.5 (dashed red line) for the AFM case and $J^*/J = +0.5$, $+1.0$, and $+1.5$ for the FM case. The inset to (b) shows the magnetization of several important planes in the FM film. The near-surface magnetic moments in FM systems are reduced, in exactly the same manner as in the AFM case.

of the external field, which acts upon all planes equally, increases the magnetization of odd-numbered planes (which have positive m), and decreases that of the even-numbered planes (which have negative m). Considering that the outer planes have weaker coupling to the core of the film, they are more susceptible to the external field. The magnetic moment of the surface planes thus increases more, compared to that of the core planes. This change in the system corresponds to a reversing of the finite-size effects discussed above.

We continue by suggesting how our findings may be observed experimentally by comparing the net magnetization $M(T)$ of AFM films to the average absolute plane magnetization. The $M(T)$ curves shown in this paper represent theoretical experiments, where the vectorial sum of the plane magnetizations is projected onto a measurement axis, like in a magnetometer with small external fields. In other experiments, however, such as neutron diffraction, the magnetic intensity is the average of the absolute plane magnetization $M_{\text{neutron}}(T) = |m(T)|$. Figure 2 showed that $M(T) \neq |m(T)|$; therefore, a

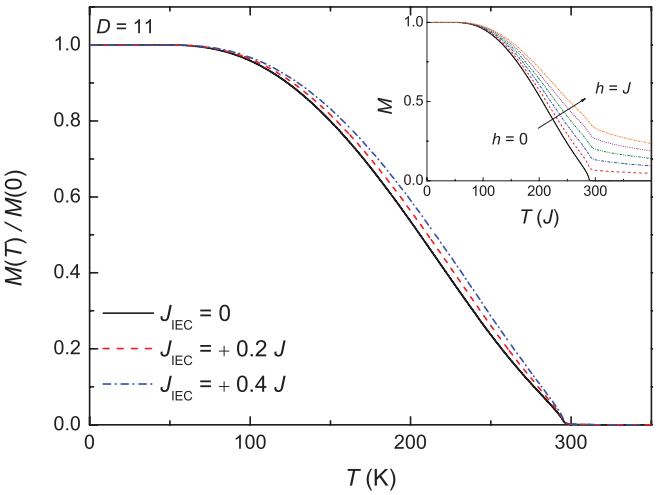

FIG. 5. (Color online) Net magnetization per film for systems with $D = 11$ and $J^* = -J$ as a function of temperature with different strengths of IEC. With increasing IEC strength $M(T)$ is enhanced; this is because the IEC acts on the surface planes, which in turn affect the near-surface planes. The inset shows the effect of the external field h on the $M(T)$ curve.

comparison of neutron diffraction intensity and low applied field magnetometry $M(T)$ should show a difference for thin film AFM's (note that it is important that the magnetometry not be dominated by ferromagnetic impurities or second phases, or by the usual paramagnetic AFM contribution). In fact, this was seen in CoO multilayers,[19] which exhibited a somewhat different temperature dependence in $M(T)$ measured in a magnetometer and the normalized neutron diffraction data, most visible near $T = 0.5T_N$. Such a comparison can therefore be used to estimate the finite-size effects including surfaces and grain boundaries in metal oxide AFM films and multilayers and probe the extent to which surface magnetization is reduced in such low-dimensional oxide antiferromagnets. Most importantly, the inequality $M(T) \leqslant |m(T)|$ is valid for any AFM film regardless of the interaction parameters in the system. For any set of interaction strengths $J > 0$ and $J^* < 0$ the net magnetization of an AFM film will always be lower than the average plane magnetization, or the magnetization of any single uncompensated plane.

We note finally that the simulations in this work were done assuming perfect crystalline planes with full atomic occupancy. In the case of defects or grain boundaries in real systems the number of uncompensated spins increases drastically and may produce similar effects as the ones found here. In addition, however, uncoupled spins, e.g., on rough surfaces or corners, can exhibit *paramagnetic* behavior which can strongly influence the $M(T)$ curve of the films in the presence of an external field.

IV. CONCLUSIONS

We have simulated antiferromagnetic thin films with thicknesses of up to 11 crystalline planes using mean-field approximation. Our study showed that films with an even number of planes have zero magnetization at all temperatures, whereas odd-numbered systems exhibit ferromagnetism due

to unequal magnetization of near surface layers, where the net magnetization of the film is lower than that of any single uncompensated plane at intermediate temperatures. With increasing film thickness the Néel temperature increases monotonically and reaches the bulk value after a few planes, while the form of the $M(T)$ curve is dramatically changed due to finite-size effects at near-surface planes which dominate AFM films despite having little effect on FM films due to compensation. The difference between near-surface magnetization and the core of the film changes strongly with interplane coupling: with smaller J^* it becomes smaller because the energy difference between near-surface and core planes becomes lower, and vice versa. We also found that turning on a positive interlayer exchange coupling inhibits these finite-size effects and promotes ferromagnetism in odd numbered systems by increasing the surface magnetization, whereas negative IEC results in zero net magnetization due to full cancellation of magnetic moments in a multilayer. Finally, we showed how these effects can be observed experimentally by comparing temperature-dependent magnetization measurements and neutron diffraction experiments.

ACKNOWLEDGMENTS

We gratefully acknowledge funding from the Swiss National Science Foundation via Grant No. PBEZP2-142894 (M.C.) and by the US Department of Energy, Office of Science, Office of Basic Energy Sciences, Division of Materials Sciences and Engineering under Contract No. DE-AC02-05CH11231 (F.H.).

*Corresponding author: charilaou@berkeley.edu

[1] F. Aguilera-Granja and J. L. Morán-López, Solid State Commun. **74**, 155 (1990).
[2] P. J. Jensen, H. Dreyssé, and K. H. Bennemann, Surf. Sci. **269/270**, 627 (1992).
[3] O. Hjortstam, J. Trygg, J. M. Wills, B. Johansson, and O. Eriksson, Phys. Rev. B **53**, 9204 (1996).
[4] A. Ney, P. Poulopoulos, and K. Baberschke, Europhys. Lett. **54**, 820 (2001).
[5] R. Rausch and W. Nolting, J. Phys.: Condens. Matter **21**, 376002 (2009).
[6] J. J. Alonso and J. F. Fernández, Phys. Rev. B **74**, 184416 (2006).
[7] K. K. Pan, Phys. Rev. B **64**, 224401 (2001); **71**, 134524 (2005); Physica A **391**, 1984 (2012).
[8] H. T. Diep, Phys. Rev. B **43**, 8509 (1991).
[9] M. Takano, T. Terashima, Y. Bando, and H. Ikeda, Appl. Phys. Lett. **51**, 205 (1987).
[10] E. N. Abarra, K. Takano, F. Hellman, and A. E. Berkowitz, Phys. Rev. Lett. **77**, 3451 (1996).
[11] T. Ambrose and C. L. Chien, Phys. Rev. Lett. **76**, 1743 (1996).
[12] Y. J. Tang, D. J. Smith, B. L. Zink, F. Hellman, and A. E. Berkowitz, Phys. Rev. B **67**, 054408 (2003).
[13] W. H. Meiklejohn and C. P. Bean, Phys. Rev. **105**, 904 (1957).
[14] M. N. Baibich, J. M. Broto, A. Fert, F. Nguyen Van Dau, F. Petroff, P. Etienne, G. Creuzet, A. Friederich, and J. Chazelas, Phys. Rev. Lett. **61**, 2472 (1988).
[15] C. G. Shull, W. A. Strauser, and E. O. Wollan, Phys. Rev. **83**, 333 (1951).
[16] J. Kanamori, Prog. Theor. Phys. (Japan) **17**, 177 (1957); **17**, 197 (1957).
[17] W. L. Roth, Phys. Rev. **110**, 1333 (1958).
[18] R. M. Cornell and U. Schwertmann, *The Iron Oxides* (John Wiley & Sons Ltd, New York, 2003).
[19] H.-J. Lee, C. Bordel, J. Karel, D. W. Cooke, M. Charilaou, and F. Hellman, Phys. Rev. Lett. **110**, 087206 (2013).
[20] K. Binder and P. C. Hohenberg, Phys. Rev. B **9**, 2194 (1974).
[21] D. P. Landau and K. Binder, J. Magn. Magn. Mater. **104–107**, 841 (1992).
[22] W. Nolting and C. Santos, Physica B **321**, 189 (2002).
[23] Y. Laosiritaworn, J. Poulter, and J. B. Staunton, Phys. Rev. B **70**, 104413 (2004).
[24] N. M. Mermin and H. Wagner, Phys. Rev. Lett. **17**, 1133 (1966).
[25] A. Gelfert and W. Nolting, Phys. Status Solidi B **217**, 805 (2000).
[26] R. Agra, F. van Wijland, and E. Trizac, Eur. J. Phys. **27**, 407 (2006).
[27] M. Charilaou, K. K. Sahu, A. U. Gehring, and J. F. Löffler, Phys. Rev. B **86**, 104415 (2012).
[28] M. B. Salamon, Phys. Rev. B **2**, 214 (1970).
[29] S. Zhang and G. Zhang, J. Appl. Phys. **75**, 6685 (1994).
[30] V. Staemmler and K. Fink, Phys. Chem. **278**, 79 (2002).
[31] W. Haubenreisser, W. Brodkorb, A. Corciovei, and G. Costache, Phys. Status Solidi **53**, 9 (1972).
[32] P. M. Levy, S. Maekawa, and P. Bruno, Phys. Rev. B **58**, 5588 (1998).
[33] L. Néel, Ann. Phys. (Paris) **3**, 137 (1948).
[34] M. Stampanoni, A. Vaterlaus, M. Aeschlimann, and F. Meier, Phys. Rev. Lett. **59**, 2483 (1987).
[35] M. Stampanoni, Appl. Phys. A **49**, 449 (1989).
[36] C. Liu and S. D. Bader, J. Appl. Phys. **67**, 5758 (1990).
[37] Y. Li and K. Baberschke, Phys. Rev. Lett. **68**, 1208 (1992).
[38] E. Schierle, E. Weschke, A. Gottberg, W. Söllinger, W. Heiss, G. Springholz, and G. Kaindl, Phys. Rev. Lett. **101**, 267202 (2008).